

Comparison of BRDF-Predicted and Observed Light Curves of GEO Satellites

Angelica Cenicerros, David E. Gaylor
University of Arizona

Jessica Anderson, Elfego Pinon III
Emergent Space Technologies, Inc.

Phan Dao
AFRL/RV

Richard Rast
AFRL/RD

Although the amount of light received by sensors on the ground from Resident Space Objects (RSOs) in geostationary orbit (GEO) is small, information can still be extracted in the form of light curves (temporal brightness or apparent magnitude). Previous research has shown promising results in determining RSO characteristics such as shape, size, reflectivity, and attitude by processing simulated light curve data with various estimation algorithms. These simulated light curves have been produced using one of several existing analytic Bidirectional Reflectance Distribution Function (BRDF) models. These BRDF models have generally come from researchers in computer graphics and machine vision and have not been shown to be realistic for telescope observations of RSOs in GEO. While BRDFs have been used for SSA analysis and characterization, there is a lack of research on the validation of BRDFs with regards to real data. In this paper, we compared telescope data provided by the Air Force Research Laboratory (AFRL) with predicted light curves from the Ashikhmin-Premoze BRDF and two additional popular illumination models, Ashikhmin-Shirley and Cook-Torrance. We computed predicted light curves based on two line mean elements (TLEs), shape model, attitude profile, observing ground station location, observation time and BRDF. The predicted light curves were then compared with AFRL telescope data. The selected BRDFs provided accurate apparent magnitude trends and behavior, but uncertainties due to lack of attitude information and deficiencies in our satellite model prevented us from obtaining a better match to the real data. The current findings present a foundation for ample future research.

1. BACKGROUND

Bidirectional reflectance distribution functions are used to estimate the amount of incident light which is reflected by an object and is defined as the sum of the specular and diffuse reflections, which are functions of its material properties, as well as the angles of incidence and reflection of incoming light. BRDFs can be used to model brightness, which is highly dependent on shape and attitude, of an RSO as seen from the ground. When defining reflected light from a surface for a particular BRDF, one must consider the direction of the incoming light source \hat{L} , the direction of the observer \hat{V} , the halfway vector \hat{H} between the light source and the observer, and the surface normal direction \hat{N} . These vectors are shown in Fig. 1 along with the angles used to define their orientation.

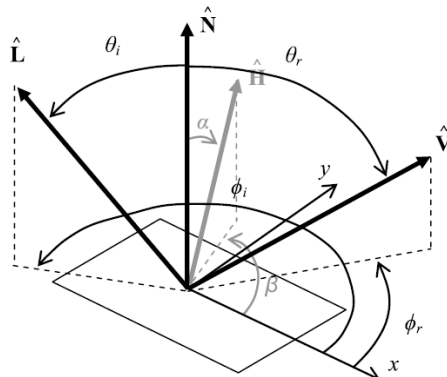


Figure 1 BRDF Reflection Vectors [1]

There have been few attempts to compare results from distinct BRDFs with the data obtained through telescope observations of RSOs. This comparison would allow us to further understand these illumination models and their ability to predict observed brightness. This paper compares estimated light curves from three distinct BRDFs, Ashikhmin-Premoze, Ashikhmin-Shirley, and Cook-Torrance, models originally presented in [1][2][3], with real telescope data. By propagating a set of RSOs through a specified time range as viewed from a particular observation station, simulated apparent magnitude was calculated and compared to the observed apparent magnitude from that station. This research analyzes how well each BRDF models the real data and also provides an opportunity to compare the precision of the three selected models with each other.

2. AFRL-PROVIDED TELESCOPE DATA

The AFRL Space Vehicles Directorate provided a set of telescope observations captured over 18 years from five different observation stations: Kirtland Raven, Dayton Raven, RME Raven, U.S. Air Force Academy (USAF) Mobile Plentywood, and USAFA Campus. Observations of the following five GEO satellites were selected for analysis: DirecTV4s, DirecTV8, DirecTV9s, Galaxy14, and SES-1. These satellites were chosen because some information on their shape and size was provided to us. This data is displayed in Table 1. In this table, SSN stands for Space Surveillance Network and SP stands for solar panel. The data included observations ranging from 1996 to 2013, depending on the analyzed RSO; however, this research focused on RSO observations collected in the year 2013. The provided data included information such as hour angle, phase angle, and range and also included more than one observation station per RSO. Our work analyzed the observations gathered from only one station for a specific RSO. It must be noted that the data provided to us by AFRL did not include attitude information of the RSOs which required us to assume the satellites were nadir-pointing with unknown orientation about the nadir direction.

Table 1 RSO Basic Information and Dimensions

Satellite	SSN#	Longitude	Body Width (m)	Body Height (m)	Body Depth (m)	# SPs	SP width (m)	Each SP Total Length (m)
DTV-4S	26985	101.15 W	3.4	2.9	7.5	2	2.16	10.16
DTV-8	28659	100.81 W	3.4	2.9	2	2	2.5	12
DTV-9s	29494	101.08 W	3.4	2.9	7.9	2	2.5	12
Galaxy 14	28790	124.96 W	4.2	4.2	4.2	2	4.3	8.6
SES-1	36516	101 W	1.7	1.7	2.9	2	1.2	5.2

3. BRDF MODELS

In order to predict an RSO’s apparent magnitude as observed from Earth, the RSO is modeled as a system consisting of n flat plates, all of which reflect a certain amount of light. This reflected light is characterized by BRDFs. A BRDF model determines the reflection and distribution of light energy from a specified surface. The two directions of interest for the BRDF are the direction from which the light source originates and the one in which it reflects from the surface. The direction of reflectivity, once the light has struck a surface, is the one which the viewer perceives. There are numerous BRDF designs that could provide feasible illumination models; however, the analysis in this paper focused on three individual BRDF models: Ashikhmin-Premoze, Ashikhmin-Shirley, and Cook-Torrance.

The simulation was originally set up with the Ashikhmin-Premoze BRDF, which is a modified, simplified version of the Ashikhmin-Shirley illumination model. The Ashikhmin-Premoze BRDF differs from the Ashikhmin-Shirley model mainly in that it simplifies the denominator of the specular term, and it allows for the use of an arbitrary normalized function $p(h)$ instead of a specific anisotropic Phong function [2]. The Ashikhmin-Premoze BRDF was selected for implementation in the original simulation due to its spectral reflectance term being amenable to computation of the analytic Jacobian of the measurements.

The other two models included in the simulation for this light-curve analysis, Ashikhmin-Shirley and Cook-Torrance, are commonly used BRDF models in computer graphics that have been shown to provide accurate representations of their intended visual target. All three BRDF models incorporate diffuse and specular reflectivity terms. While the specular term consists of the light reflected in a specific direction, as displayed in Fig. 2, the diffuse term is composed of randomly scattered light, as shown in Fig. 3.

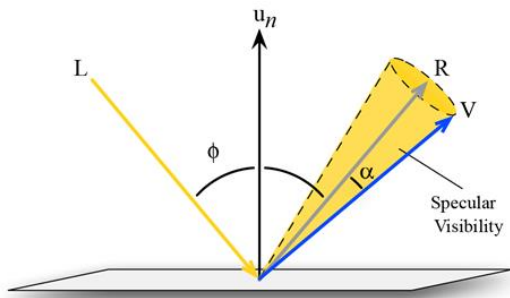


Figure 2 Specular Reflection

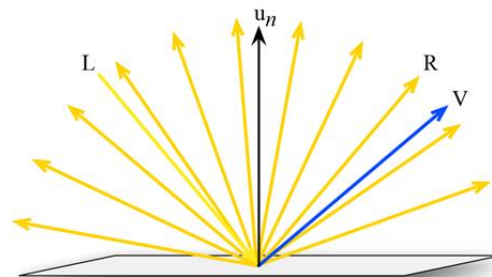


Figure 3 Diffuse Reflection

3.1 Ashikhmin-Shirley and Ashikhmin-Premoze BRDFs

Ashikhmin-Shirley is an anisotropic BRDF model which provides good modeling of metals and plastics, along with general purpose surfaces, and utilizes a Fresnel term to evaluate specular reflectivity. However, unlike Cook-Torrance, Ashikhmin-Shirley's model has been adapted in order to conserve energy through the implementation of a non-Lambertian diffuse term [3]. It is computationally expensive to evaluate, but due to its useful properties and intuitive parameters, the Ashikhmin-Shirley model was selected as one of the BRDF methods for this research. Equations 1 and 2 display the specular and diffuse components of the Ashikhmin-Shirley BRDF, respectively. The specular term consists of the two parameters n_u and n_v , two Phong-like exponents which control the shape of the specular lobe [3]. For this research, n_u is equal to n_v . R_d and R_s are parameters which specify the "specular reflectance at normal incidence" and the "diffuse reflectance of the 'substrate' under the specular coating," respectively [3]. The F term, as evaluated by Eq. 3, is Schlick's approximation to the Fresnel fraction [3]. In the Fresnel term, F_0 is material's reflectance at normal incidence [3]. As a note, while the Ashikhmin-Shirley uses Eq. 1 for its specular calculation, the Ashikhmin-Premoze changes the denominator term $(\hat{V} \cdot \hat{H}) \max((\hat{N} \cdot \hat{L}), (\hat{N} \cdot \hat{V}))$ to $\hat{N} \cdot \hat{L} + \hat{N} \cdot \hat{V} - (\hat{N} \cdot \hat{L}), (\hat{N} \cdot \hat{V})$ [2].

$$\rho_s(\hat{L}, \hat{V}) = \frac{\sqrt{(n_u+1)(n_v+1)} (\hat{N} \cdot \hat{H})}{8\pi (\hat{V} \cdot \hat{H}) \max((\hat{N} \cdot \hat{L}), (\hat{N} \cdot \hat{V}))} \frac{(n_u(\hat{H} \cdot \hat{u})^2 + n_v(\hat{H} \cdot \hat{v})^2)}{(1 - (\hat{N} \cdot \hat{H})^2)} F(\hat{V} \cdot \hat{H}) \quad (1)$$

$$\rho_d(\hat{L}, \hat{V}) = \frac{28R_d}{23\pi} (1 - R_s) \left(1 - \left(1 - \frac{(\hat{N} \cdot \hat{L})}{2}\right)^5\right) \left(1 - \left(1 - \frac{(\hat{N} \cdot \hat{V})}{2}\right)^5\right) \quad (2)$$

$$F = F_0 + \left(\frac{1}{5} - F_0\right) (1 - \hat{V} \cdot \hat{H})^5 \quad (3)$$

3.2 Cook-Torrance BRDF

The Cook-Torrance lighting model is one that is acceptable for a wide range of objects, being a general model for handling rough material surfaces. Like the Ashikhmin-Shirley model, the Cook-Torrance method consists of diffuse and specular terms, as defined by Eq. 4 and 5, respectively. It is also computationally expensive to evaluate, although the complexity behind the Cook-Torrance method allows for a more accurate and physically-based specular reflection value through the use of a model specific Fresnel reflectance term. Looking at the diffuse term presented in Eq. 4, ρ is the diffuse reflectance, which is a value between 0 and 1 [1]. The specular term of the Cook-Torrance model consists of a microfacet distribution term (Eq. 6), a geometric term (Eq. 7), and a Fresnel term (Eq. 8). The distribution term provides information on the orientation of the microfacets, with similar orientations on smooth surfaces and more diverse orientations on rough surfaces. This research used the Beckmann distribution, seen in Eq. 6, as the microfacet distribution term, where α is the angle between \hat{N} and \hat{H} . The geometric factor allows for the inclusion of shadowing and self-masking effects between the microfacets, and the Fresnel term, similar to the one observed with the Ashikhmin-Shirley model, provides the specular reflection value, telling us which portion of the light was reflected and which other was transmitted. [4]

$$R_d = \frac{\rho}{\pi} \quad (4)$$

$$R_s = \frac{FDG}{\pi(\hat{N} \cdot \hat{L})(\hat{N} \cdot \hat{V})} \quad (5)$$

$$D = \frac{e^{-\left[\frac{\tan \alpha}{m}\right]^2}}{\pi m^2 (\cos \alpha)^4} \quad (6)$$

$$G = \min \left\{ 1, \frac{2(\hat{N} \cdot \hat{H})(\hat{N} \cdot \hat{V})}{(\hat{V} \cdot \hat{H})}, \frac{2(\hat{N} \cdot \hat{H})(\hat{N} \cdot \hat{L})}{(\hat{V} \cdot \hat{H})} \right\} \quad (7)$$

$$F = \frac{(g - \hat{V} \cdot \hat{H})^2}{2(g + \hat{V} \cdot \hat{H})^2} \left\{ 1 + \frac{[(\hat{V} \cdot \hat{H})(g + \hat{V} \cdot \hat{H}) - 1]}{(\hat{V} \cdot \hat{H})(g - \hat{V} \cdot \hat{H}) + 1} \right\} \quad (8)$$

$$g^2 = n^2 + (\hat{V} \cdot \hat{H})^2 - 1 \quad (9)$$

$$n = \frac{1 + \sqrt{F_0}}{1 - \sqrt{F_0}} \quad (10)$$

4. SIMULATION CONFIGURATION

To test the BRDF models, information on each of the RSOs was included in a MATLAB script and processed by a measurement generating function. This function's purpose is to simulate observations based on the specified object's provided properties. In this case, the observation time, initial TLE, estimated shape model, expected attitude and size, among other parameters, were incorporated into the simulation for each RSO and processed by the measurement generating function. Assumptions were made based on basic knowledge or online research of each RSO in order to successfully incorporate it into the simulation. Therefore, discrepancies were expected between the simulated and actual data due to the lack of detailed available information on features such as attitude, absolute size of the RSOs, and exact TLEs during the propagation time. This research assumed nadir-pointing orientation for all of the RSOs, but rotation of the RSO about the nadir was required to find the best fit with the real data. This orientation approximation as well as the limited accuracy of the TLEs are the driving factors for the uncertainty in our models.

By including each RSO's information, propagating the data for a specific time, and then comparing the results with the actual observed data, we were able to determine how accurately the BRDF models approximate reality. The data was processed using the three described BRDF models, Ashikhmin-Premoze, Ashikhmin-Shirley, and Cook Torrance, providing a range of apparent magnitudes of each RSO for the selected time frame. The resulting apparent magnitude was then compared with the collected apparent magnitude values provided by AFRL.

5. RESULTS

Apparent magnitude plots comparing the output from the three distinct BRDF models with the real apparent magnitude can be seen in Fig. 4 through 31 below. There is one plot per BRDF, three total per RSO (except for DirecTV4s and DirecTV8 which include 2 plots per BRDF, 6 per RSO). A second plot for both DirecTV4s and DirecTV8 is included because these satellites were observed over two distinct time periods. The plot or plots for each RSO contain the same real data across the three illumination models. For example, looking at DIRECTV4s, Fig. 4 displays the same real observation data as Fig. 6 and Fig. 8. The difference between these plots is the apparent magnitude values simulated using each BRDF.

Also, two separate observation tracks can be seen in the majority of the plots. Although there is fluctuation of values from one observation to another, the primary reason for these two lines is the inclusion of a second color filter when collecting the apparent magnitude values. Therefore, each line would represent the apparent magnitude values observed by two distinct color filters (blue and red, with the red filter corresponding to the consistently lower apparent magnitude value line). However, the observation times for each filter are not the same, meaning that each observation has its own unique time stamp. All the results from Figures 4 to 31 show two green observation trend lines, some figures more distinctly than others. For all of these plots, the higher value green trend line represents the apparent magnitude observations coming from the blue filter, while the lower value green trend line comes from the red filter.

Studying the results, one can see that the Cook-Torrance BRDF agrees more closely with the observed data, staying within the value range of the real data. The second best results were given by the Ashikhmin-Shirley BRDF, and the least accurate apparent magnitude came from the Ashikhmin-Premoze model. A notable exception for this trend is observed in Galaxy 14, where Ashikhmin-Premoze performed within the accuracy range of the Cook-Torrance model. For the other RSOs, the Ashikhmin-Premoze BRDF tended to predict higher-than-actual apparent magnitude, indicating that the modeled RSO reflected less light than the actual RSO.

5.1 DIRECTV4S

Simulations for DirecTV4s were created for two time intervals, each time window with a particular observation station. The results from Fig. 4, 6, 8, and 10 were collected from the Kirtland Raven station while Fig. 5, 7, 9 and 11 came from the USAFA Campus station. The plots show that the three BRDFs are able to detect the general path of the apparent magnitude, but the Cook-Torrance illumination model proved to not only better follow the trend but also better estimate the real data values. The performance of each BRDF is best examined in Fig. 10 and 11.

Some of the AFRL-provided observations included solar panel glints, which can be observed as sudden high peaks of apparent magnitude values, and one such glint is seen in the DirecTV4s plots from the USAFA Campus station. The BRDF models approximated this peak; the Cook-Torrance model was the most successful at capturing the glint.

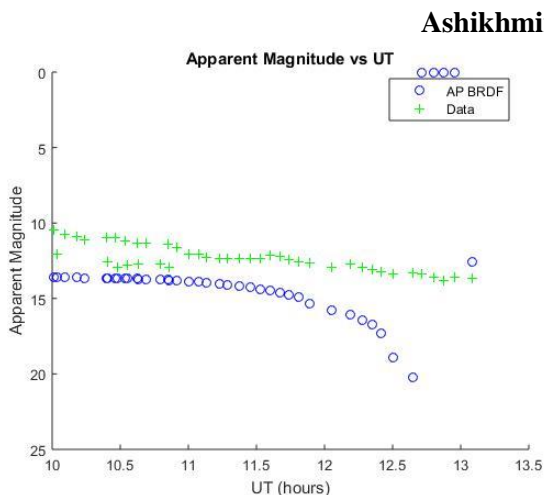


Figure 4 DTV4S Ashikhmin-Premoze vs. Real Data Set 1
 Top green line: Red filter, bottom green line: Blue filter

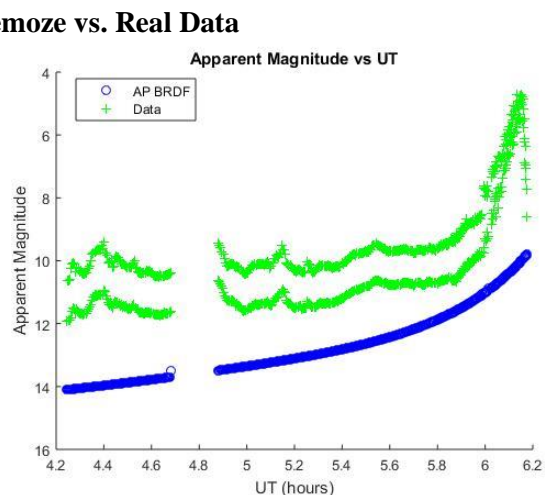


Figure 5 DTV4S Ashikhmin-Premoze vs. Real Data Set 2
 Top green line: Red filter, bottom green line: Blue filter

Ashikhmin-Shirley vs. Real Data

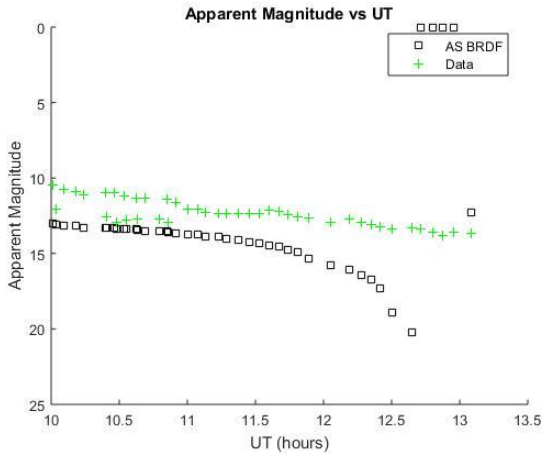


Figure 6 DTV4S Ashikhmin-Shirley vs. Real Data Set 1
Top green line: Red filter, bottom green line: Blue filter

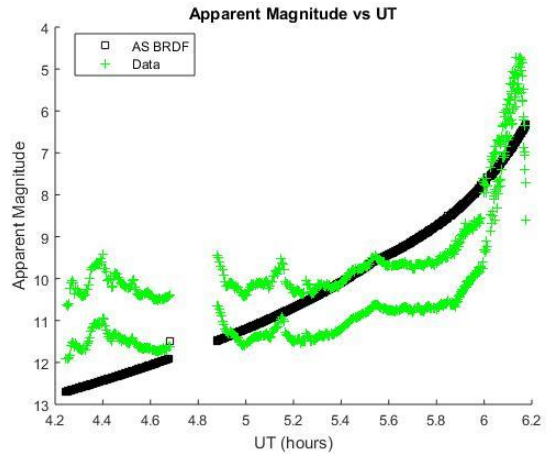


Figure 7 DTV4S Ashikhmin-Shirley vs. Real Data Set 2
Top green line: Red filter, bottom green line: Blue filter

Cook-Torrance vs. Real Data

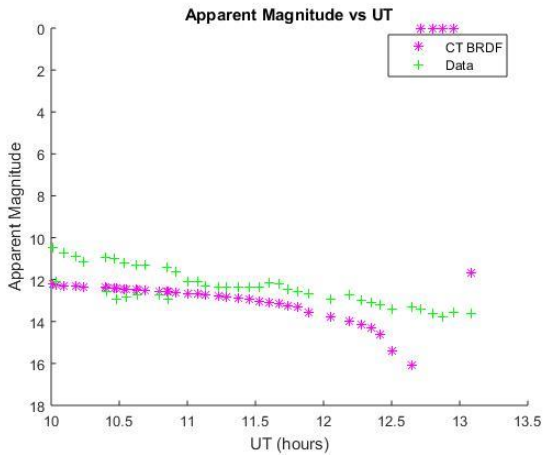


Figure 8 DTV4S Cook-Torrance vs. Real Data Set 1
Top green line: Red filter, bottom green line: Blue filter

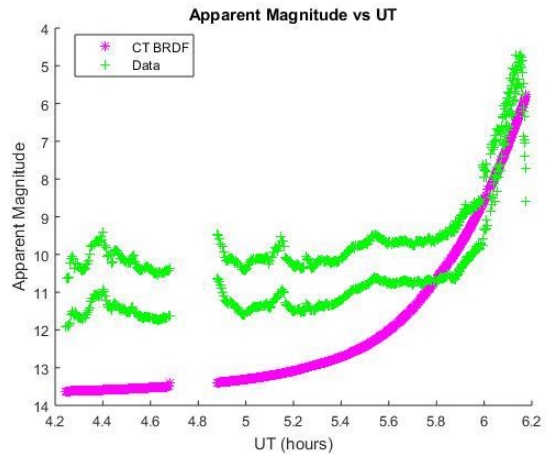


Figure 9 DTV4S Cook-Torrance vs. Real Data Set 2
Top green line: Red filter, bottom green line: Blue filter

DTV4S Predicted vs Real Data

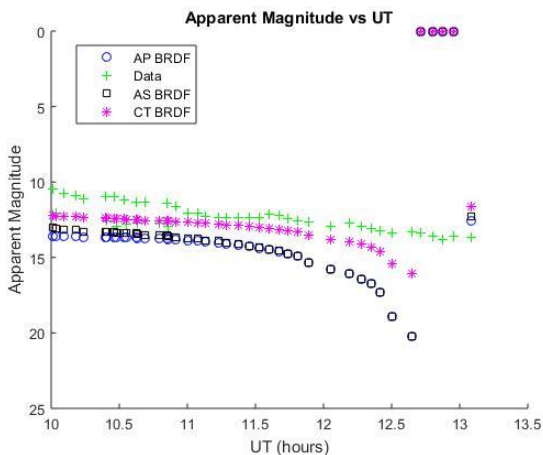


Figure 410 DTV4S Predicted vs Real Data Set 1
Top green line: Red filter, bottom green line: Blue filter

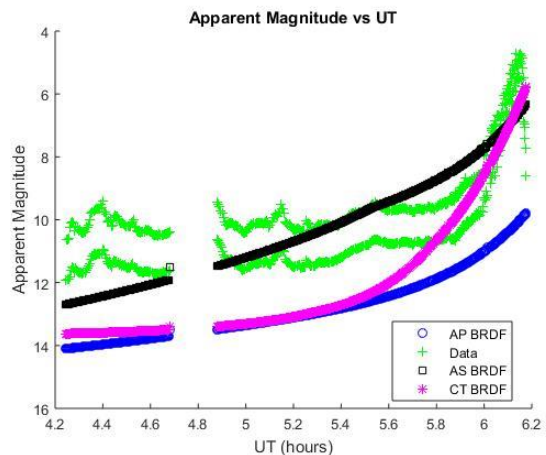


Figure 511 DTV4S Predicted vs Real Data Set 2
Top green line: Red filter, bottom green line: Blue filter

5.2 DIRECTV8

Simulations for DirecTV8 were created for two time intervals from the Dayton Raven observation station. Figures 12 through 19 show that the three BRDFs are able to detect the general path of the apparent magnitude, but the Cook-Torrance illumination model proved to best match the data values. Ashikhmin-Shirley results also provided an acceptable approximation while Ashikhmin-Premoze clearly presents the most erroneous results. The performance of each BRDF is best examined in Fig. 18 and 19.

Similar to DirecTV4s, a sudden high peak of apparent magnitude values indicates a solar panel glint. However, unlike with the DirecTV4s results, none of the BRDF models properly model this peak.

Ashikhmin-Premoze vs. Real Data

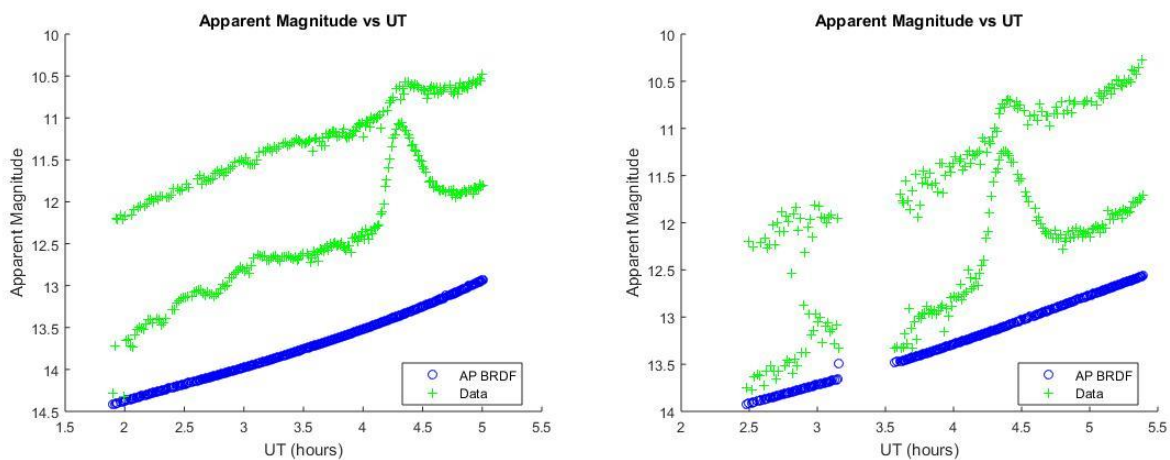


Figure 612 DTV8 Ashikhmin-Premoze vs. Real Data Set 1 Figure 713 DTV8 Ashikhmin-Premoze vs. Real Data Set 2
 Top green line: Red filter, bottom green line: Blue filter Top green line: Red filter, bottom green line: Blue filter

Ashikhmin-Shirley vs. Real Data

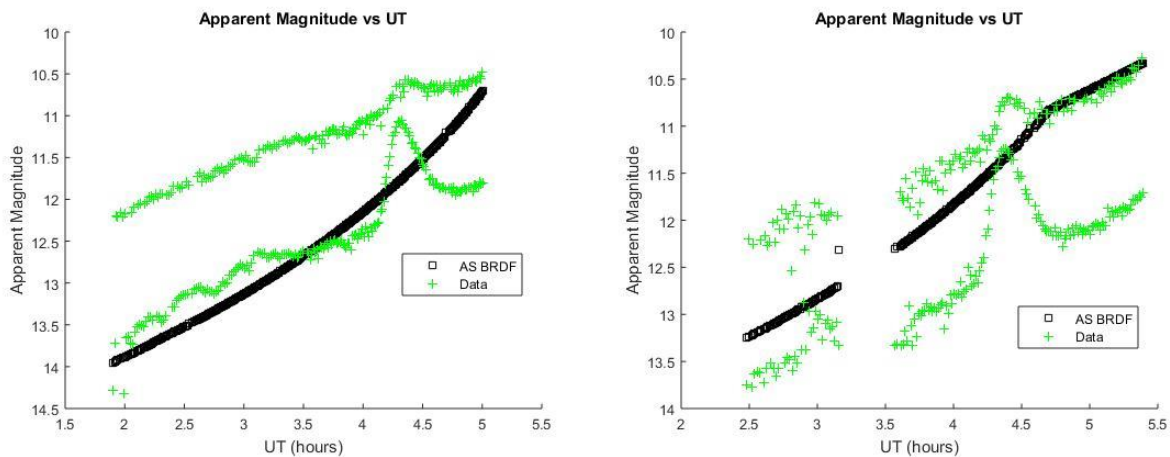


Figure 814 DTV8 Ashikhmin-Shirley vs. Real Data Set 1 Figure 915 DTV8 Ashikhmin-Shirley vs. Real Data Set 2
 Top green line: Red filter, bottom green line: Blue filter Top green line: Red filter, bottom green line: Blue filter

Cook-Torrance vs. Real Data

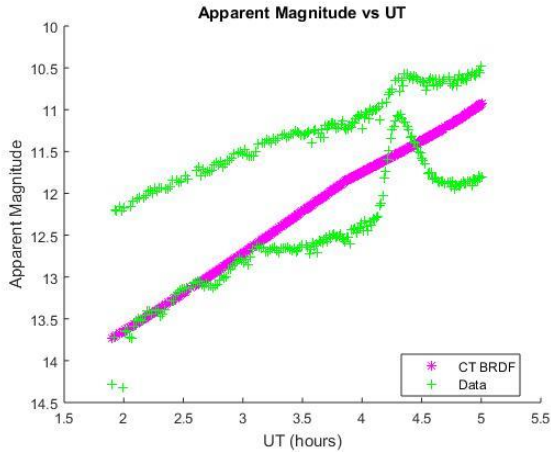


Figure 1016 DTV8 Cook-Torrance vs. Real Data Set 1

Top green line: Red filter, bottom green line: Blue filter

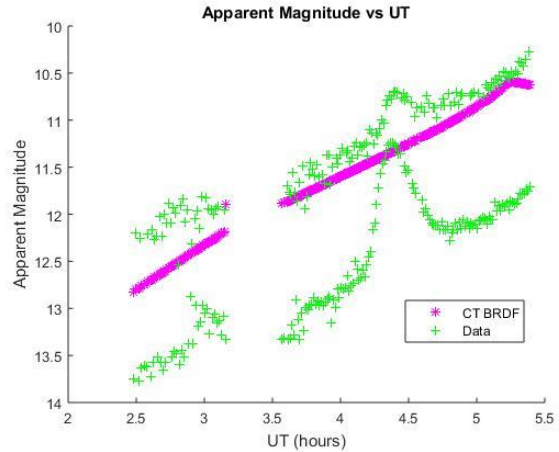


Figure 1117 DTV8 Cook-Torrance vs. Real Data Set 2

Top green line: Red filter, bottom green line: Blue filter

DTV8 Predicted vs. Real Data

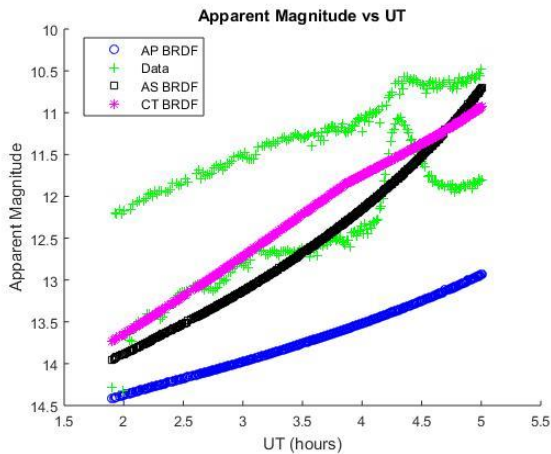


Figure 1248 DTV8 Predicted vs. Real Data Set 1

Top green line: Red filter, bottom green line: Blue filter

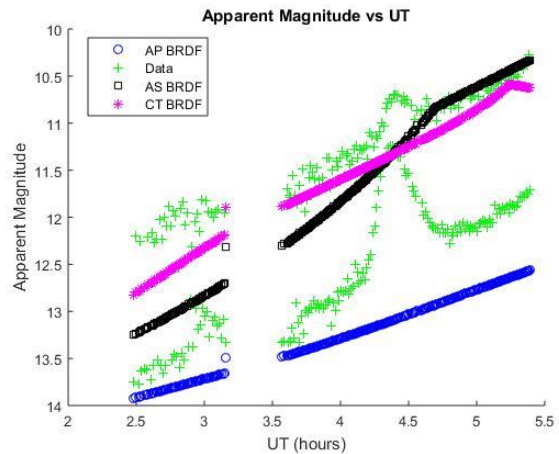


Figure 1349 DTV8 Predicted vs. Real Data Set 2

Top green line: Red filter, bottom green line: Blue filter

5.3 DIRECTV9s

Simulations for DirecTV9s were created for one time interval from the Dayton Raven observation station. Figures 20 through 23 show that the three BRDFs are able to detect the general path of the apparent magnitude, but the Cook-Torrance illumination model proved to best match the data values and direction. Ashikhmin-Shirley results also provided an acceptable approximation, albeit with

some irregularities in the general value trend, while Ashikhmin-Premoze clearly presents the most erroneous results. The performance of each BRDF is best examined in Fig. 23.

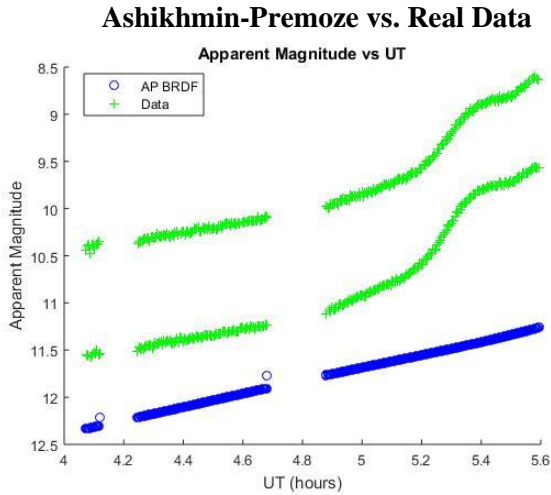


Figure 1420 DTV9s Ashikhmin-Premoze vs. Real Data
Top green line: Red filter, bottom green line: Blue filter

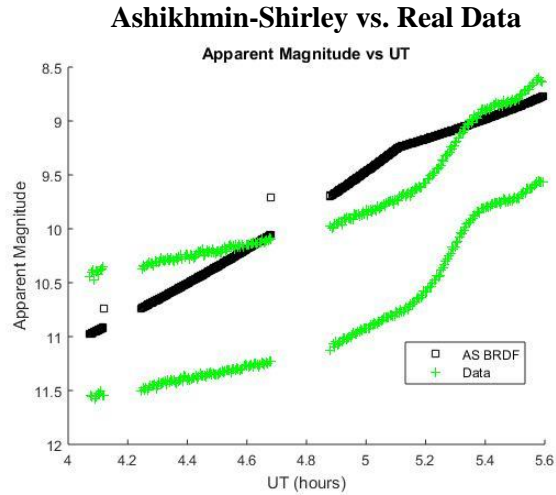


Figure 1524 DTV9s Ashikhmin-Shirley vs. Real Data
Top green line: Red filter, bottom green line: Blue filter

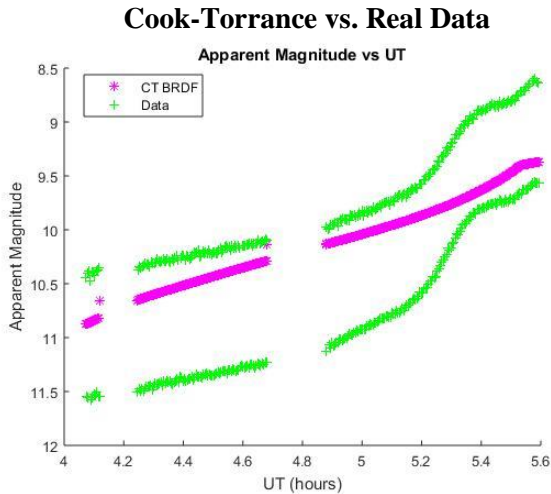


Figure 1622 DTV9s Cook-Torrance vs. Real Data
Top green line: Red filter, bottom green line: Blue filter

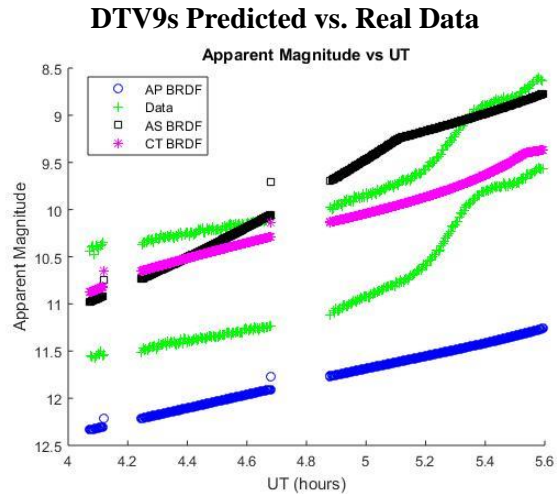


Figure 1723 DTV9s Predicted vs. Real Data
Top green line: Red filter, bottom green line: Blue filter

5.4 GALAXY14

Simulations for Galaxy 14 were created for one time interval from the RME Raven observation station. Figures 24 through 27 show that the three BRDFs are able to detect the general path of the apparent magnitude, but the Cook-Torrance illumination model proved to best match the data values and direction. Ashikhmin-Premoze results also provided an acceptable approximation while

Ashikhmin-Shirley results deviated the most from the truth. The performance of each BRDF is best examined in Fig. 27.

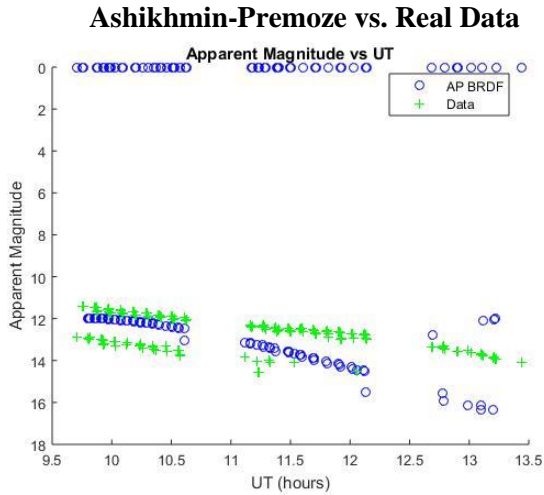


Figure 1824 Galaxy 14 Ashikhmin-Premoze vs. Real Data

Top green line: Red filter, bottom green line: Blue filter

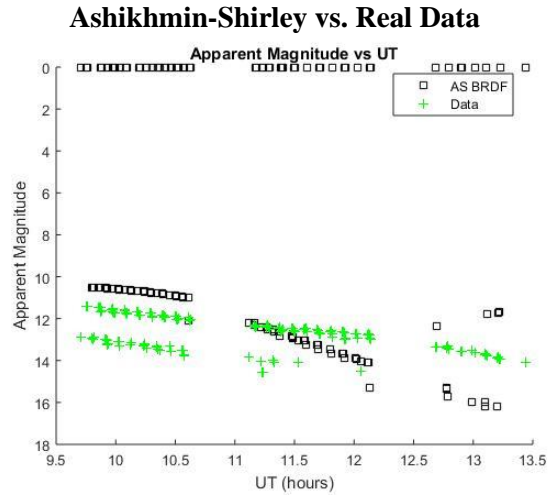


Figure 1925 Galaxy 14 Ashikhmin-Shirley vs. Real

Top green line: Red filter, bottom green line: Blue filter

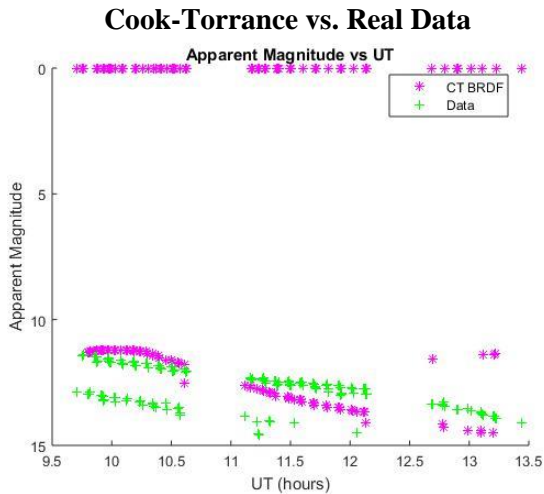


Figure 2026 Galaxy 14 Cook-Torrance vs. Real Data

Top green line: Red filter, bottom green line: Blue filter

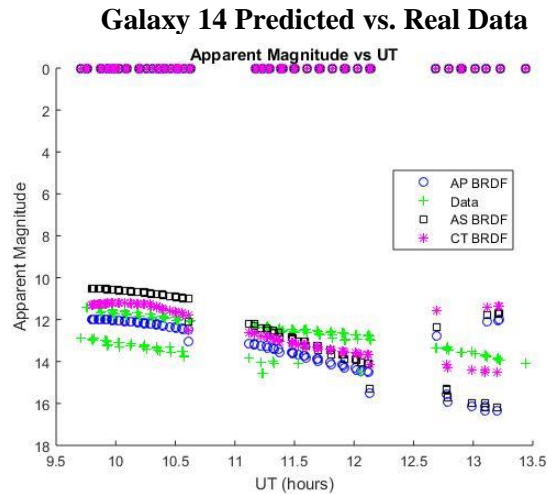


Figure 2127 Galaxy 14 Predicted vs. Real Data

Top green line: Red filter, bottom green line: Blue filter

5.5 SES-1

Simulations for SES-1 were created for one time interval from the Kirtland Raven observation station. Figures 28 through 31 show that the three BRDFs are able to detect the general path of the apparent

magnitude, but the Cook-Torrance illumination model proved to best match the data values and direction. Ashikhmin-Shirley results also presented close results while Ashikhmin-Premoze deviated the most from the real values. The performance of each BRDF is best examined in Fig. 31.

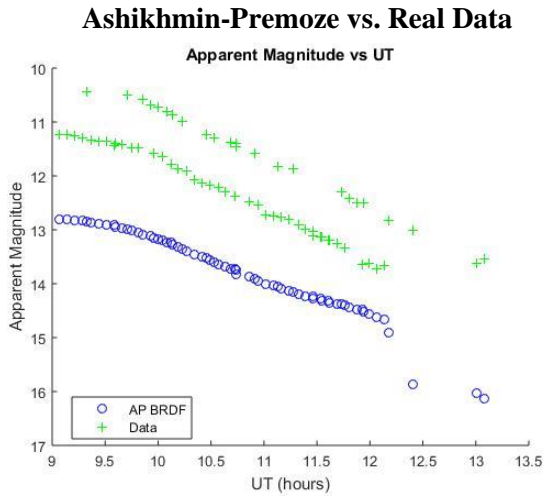


Figure 2228 SES-1 Ashikhmin-Premoze vs. Real Data

Top green line: Red filter, bottom green line: Blue filter

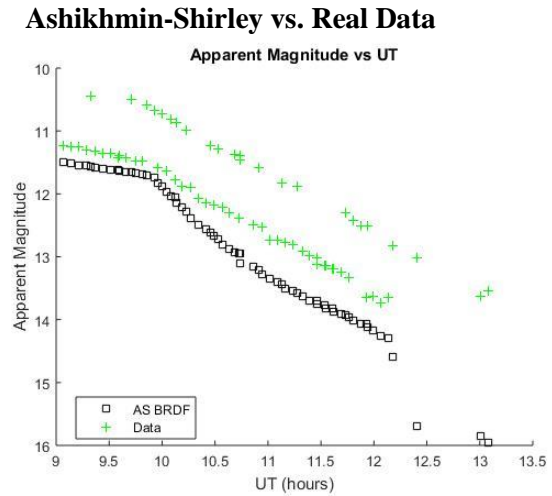


Figure 2329 SES-1 Ashikhmin-Shirley vs. Real

Top green line: Red filter, bottom green line: Blue filter

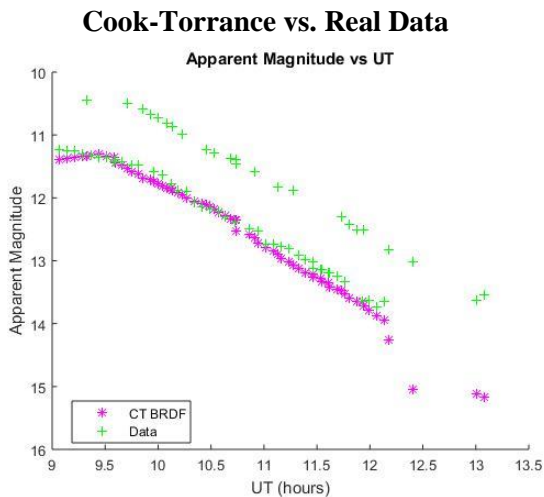


Figure 2430 SES-1 Cook-Torrance vs. Real Data

Top green line: Red filter, bottom green line: Blue filter

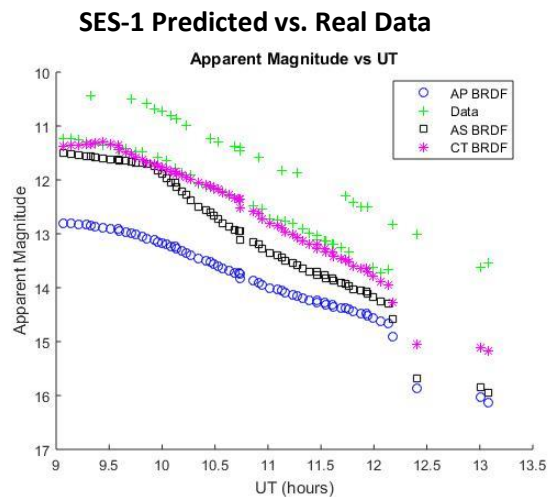


Figure 2531 SES-1 Predicted vs. Real Data

Top green line: Red filter, bottom green line: Blue filter

6. CONCLUSIONS AND FUTURE WORK

In general, our results showed that out of the three BRDF models for this research, Cook-Torrance best approximated the apparent magnitude trends and values obtained from the telescope data. The

Ashikhmin-Shirley BRDF was the next most accurate at correctly matching the real data while the Ashikhmin-Premoze model came last. However, due to the lack of knowledge of the attitude and size of the RSOs, the BRDF results were obtained by making multiple assumptions and are, therefore, limited in their portrayal of reality. In addition, discrepancies in the model setup, such as solar panels fixed relative to the bus and excluding proper axis rotation to track the sun, also provide an explanation for the lack of precision during certain observation time windows.

Future work includes further modification of the MATLAB code to improve the representation of the shape model and its dynamics to better capture solar panel glints. Also, a quantitative study of the observation frame error and average error between the BRDF predictions and the real data for more and longer propagation windows will be conducted. In addition, we plan to observe operational GEO satellites with University of Arizona telescopes and obtain accurate ephemeris and attitude data from the satellite operators. This will allow us to remove some of the deficiencies encountered with using the AFRL data to validate the BRDF models.

7. ACKNOWLEDGEMENTS

This work was partially funded by a Phase II SBIR (FA9453-14-C-029) from the AFRL Space Vehicles Directorate. Special thanks to Andrew Dianetti for his guidance and support in the completion of this paper. We acknowledge Mr. Dan Fulcoly, Dr. Jeremy Murray-Krezan, Dr. Tamara Payne, Dr. Steve Gregory, and Ms. Amber Anderson for their contribution to the collection, processing and management of the GOLDS and GCPC data.

8. REFERENCES

- [1] Wetterer, C., Linares, R., Crassidis, J., Kelecy T., Ziebart, M., and Jah, M., "Refining Space Object Radiation Pressure Modeling with Bidirectional Reflectance Distribution Functions," *J. of Guidance, Control, and Dynamics*, Vol. 37, No.1, 2014, pp. 185-188.
- [2] Ashikhmin, M. and Premoze, S., "Distribution-based BRDFs," Unpublished Technical Report, University of Utah, 2007.
- [3] Ashikhmin, M. and Shirley, P., "An anisotropic Phong BRDF model," *J. Graph. Tools*, Vol. 5, No. 2, 2000, pp. 25-32.
- [4] R. L. Cook and K. E. Torrance. A reflectance model for computer graphics. *Computer Graphics*, 15(3):307–316, August 1981.